EXPERIMENTAL ANALYSIS OF J INTEGRAL IN THE FULL-SCALE PRESSURE VESSEL TEST

S. Sedmak*, B. Petrovski*, D. Drenić**

Full-scale tests are required for operational safety evaluation of the penstock for "Bajina Basta" Pumped Storage Hydro-electric Plant, made of SUMITEN 80P HSLA steel by welding. In the burst test and hydro-pressure overloading test, previously carried out with a penstock prototype in the form of a pressure vessel, high overall resistance of the penstock had been shown. Additionally, J integral 3 pt bend tests were used for residual strength prediction of the prototype with an axial crack. J integral direct measurements in tensile panels and on a pressure vessek full-scale model with an axial crack enabled further improvement in residual strength prediction.

INTRODUCTION

The application of high strength, low alloyed (HSLA) steel in modern design of structures, exposed to high internal fluid pressure (such as pressure vessel, storage tank, penstock, pipe line) requires the evidence of operational safety under real loading condition. The operational safety is affected by different effects and their significance must be recognized for design of welded pressurized structures with minimum material consumption. First of all, the heterogeneity of weldments properties has to be considered. In the case of HSLA steel, undermatched welding consumables can be required for cold cracking avoidance, Satoh and Toyoda (1). This leads to the weld metal (WM), which will exhibit lower tensile properties compared to the base metal (BM) as it is the case with the investigated welded joints, made of SUMITEN 80P (SM 80P), a HSLA steel produced by "Sumitomo" - Japan. Secondly, the possibility of crack existance in WM or in heat-affected-zone (HAZ) must be recognized. Thirdly, the effect of residual stresses and stress concentrations will bring irregularity in stress distribution. It is not an easy

* Faculty of Technology and Metallurgy, University of Belgrade, Yugoslavia
** Faculty of Civil Engineering, University of Niš, Yugoslavia

task to analyze all these effects at once, and, when it is possible, full-scale tests under real loading condition are required as the most appropriate for this complex analysis. On the other hand, full-scale tests are expensive and their replacement by specimen tests is desirable in many situations.

In the precedent full-scale tests of penstock segment prototype, constructed as a pressure vessel, the safety was evaluated by burst test of a cracked prototype, Rak et al (2) and by specimens analysis of overloaded prototype with no crack, Sedmak et al (3). The modern HSLA steels are designed to meet high requirement regarding the brittle fracture and this is expressed through low nil-ductility-transition (NDT) temperature and reasonably high fracture toughness (K_{Ic}) values. The same is valid for their weldments. It was shown in the performed full-scale tests that the safety of welded penstock is satisfactory regarding the brittle fracture. The overall resistance of the penstock could be evaluated as very high on the basis of the results in full-scale prototype tests. Nevertheless, these tests could not prove definitely that the stable crack growth resistance is high enough and that the required safety level of welded penstock is satisfied under real loading condition and virtual stable crack growth. This could be very important if a crack propagates through WM and HAZ.

The first attempt of stable crack growth prediction was carried out for the penstock prototype by use of J integral resistance (J_R) curves for BM and WM, obtained with three-point (3 pt) bend specimens, Ratwani et al (4). Further investigation was necessary because the stress state in 3 pt bend specimen and in full-scale pressure vessel can differ significantly. A promising approach was found in the application of the J integral direct evaluation method, performed on a tensile panel with part-through (surface) flaw, Read (5). The J_R curves, obtained by this method and by 3 pt bend tests, were used for residual strength prediction of the pressure vessel model, Sedmak and Petrovski (6). The application of the J integral direct evaluation method has been extended to the same model in order to compare the crack behaviour in specimen and in full-scale condition.

Three stages of this investigation will be presented and discussed:
- J_R curves, obtained in 3 pt bend tests, as applied to penstock prototype;
- J_R curves, obtained by J integral direct evaluation method on tensile panels and by 3 pt bend specimens, as applied to full-scale pressure vessel model;
- J integral, evaluated by the direct method, and crack behaviour in full-scale model experiments.

RESIDUAL STRENGTH PREDICTION OF PENSTOCK PROTOTYPE

The possibility of crack occurence during manufacturing or operation of the penstock required the crack growth analysis for complete evaluation of its safety. This analysis, based on crack resistance curve procedure (7), that had been extended beyond the yielding, Erdogan and Ratwani (8), was applied (4) to the penstock prototype (Fig. 1). The residual strength of the prototype and penstock could be predicted by comparing the crack driving force, resulting from internal pressure, and the material crack resistance, obtained by tests, both being expressed through J integral.

The investigated weldment of the prototype was produced in 47 mm thick plates of SM 80P steel by submerged arc welding (SAW) with US-80B wire under MF38 flux, produced by "Kobe Steel" - Japan. The yield strength was found to be σ_{YB} = 755 MPa for BM-SM 80P steel and σ_{YS} = 687 MPa for SAW-WM, and the undermatching effect could be clearly recognized. The elasticity modulus E = 207 GPa and Poisson's ratio ν = 0,3 were adopted for both BM and WM.

As the most dangerous case, the existence of an axial crack was assumed. For the residual strength prediction, the crack of a presumed length 2ℓ = 180.74 mm was supposed in BM or in WM. With this crack length, the shell parameter was found to be

$$\lambda = [12\ (1 - \nu^2)]^{\frac{1}{4}} \frac{\ell}{\sqrt{Rt}} = 0.52 \quad \ldots\ldots\ldots\ldots\ldots\ldots\ldots\ldots \quad (1)$$

for mid-section diameter 2R = 4247 mm and wall thickness t = 47 mm. For λ = 0.52 a set of crack driving force lines, expressed through $\sqrt{J}$, that corresponded to the supposed values of pressure p and $pR/t\sigma_Y$ ratio, could be plotted (Fig. 2) against the ratio a/t (crack depth a normalized by wall thickness t). The $pR/t\sigma_Y$ ratio represents the tensile (membrane) stress component $p \cdot R$, normalized by yield strength σ_Y and wall thickness t. The set of crack driving force lines can be used for both BM and WM, introducing the respective σ_{YB} or σ_{YS} value, e. g. for the ratio

$$\frac{pR}{t\sigma_Y} = 0.85 \quad \ldots\ldots\ldots\ldots\ldots\ldots\ldots\ldots\ldots\ldots\ldots\ldots\ldots\ldots \quad (2)$$

the required pressure for BM is as high as p = 142 bar and for WM p = 129.2 bar.

Material crack resistance curves were obtained in 3 pt bend test using 22.5 x 45 x 200 mm specimens for both BM and WM, following the method proposed by Sumpter and Turner (9). The resulting $\sqrt{J_R}$ - Δa curves, presented in Fig. 3, are designed according to results obtained by Glavardanov et al (10). The J_R curves for BM and WM from Fig. 3 are superimposed on Fig. 2 for two assumed a_o/t

initial values of 0.25 and 0.5, for shallow (a_0 = 11.75 mm) and deep initial crack (a_0 = 23.5 mm). It should be noted that cracks of supposed length (180.74 mm) and depth (23.5 mm or 11.75 mm) are scarcely to be expected in real penstock situation, as even smaller cracks can be easily detected.

A short discussion of results from Fig. 2 will reveal the capacity of residual strength prediction by the applied method. When the applied pressure causes a crack driving force of lower intensity than required for unstable crack propagation, very slight or no crack extension would occur, e. g. for shallow crack in BM the pressure of 142 bar ($pR/t\sigma_Y$ = 0.85) will produce no visible crack depth extension. The increase in pressure from 142 bar to 153.7 bar (tangent point A on 0.92 line) will produce the stable crack depth growth for Δa = 4.61, from 11.75 mm to 16.36 mm. The pressure of 153.7 bar or higher would produce unstable crack growth according to this analysis. In the case of shallow crack in WM, the tangent point B lies on the 0.91 line, and for σ_{YS} = 687 MPa the critical pressure amounts to 138.4 bar for stable crack growth of Δa = 5.17 mm. For deep crack in BM, tangent point A' lies on 0.85 line, and corresponding value of pressure is p = 142 bar and of crack depth extension is Δa = 9.35 mm (that means the crack will extend in a stable manner from 23.5 mm to 32.85 mm). The pressure of 124.7 bar is critical for WM (point B') and a crack will grow from 23.5 mm to 29.9 mm in a stable manner. The working pressure in penstock of p = 90.5 bar can increase to p = 120.6 bar by water hammer overloading (3) and this value is obviously lower than required for final stable crack growth, even in the most critical case of large surface flaw in WM (180.74 mm long, 23.5 mm deep), that could not be expected in real penstock weldments.

The overall evaluation of penstock safety (2); (3) is well supported by additional prediction of residual strength, inspite of more or less pronounced empirical nature of performed procedure. The discussed results can be considered as being on the safe side, because the crack growth in 3 pt bend specimen is enhanced by lower constraint compared to the pressure vessel. On the other hand, the effect of crack shape has to be taken into account, and more evidence is needed to assure that different initial crack depth taken in Fig. 2 for the same J_R curves, will not lead to unreliable results and conclusions.

J INTEGRAL DIRECT EVALUATION METHOD APPLIED FOR RESIDUAL STRENGTH PREDICTION

A new pressure vessel model (Fig. 4) was constructed by welding of 16 mm thick SM 80P steel plates for subsequent full-scale tests, and its residual strength has been predicted for the case of an axial crack, using the results obtained with flawed tensile panels for J integral direct evaluation methods and 3 pt bend tests. The introduction of flawed tensile panels and J integral direct

evaluation enabled two basic improvements compared to 3 pt bend specimens. The part-through surface crack in tensile panel can be considered as similar to the corresponding surface crack in the real pressure vessel. The direct evaluation method is based on J integral definition, and no strict limitations regarding initial crack and shape are required.

The model shell parameter $\lambda = 0.60$ is calculated for mid-section diameter 2R = 1184 mm, wall thickness t = 16 mm and the assumed crack length 2ℓ = 64.25 mm. A set of crack driving force lines is plotted in Fig. 5, as expressed by $\sqrt{J}$ integral, against the ratio a/t, for different dimensionless tensile stress components $pR/t\sigma_Y$.

Again, material crack resistance for BM and SAW WM is expressed through J_R curves, obtained with tensile panels and 3 pt bend specimens, and superimposed in Fig. 5. The initial crack depth a_o is normalized by a wall thickness t=16 mm, being the same for model, tensile panel and 3 pt bend specimen of a square cross-section 16 x 16 mm. The shape of two BM J_R curves is similar (BM-2 for tensile panel and 80-1 for 3 pt bend specimen), in spite of different initial crack shape and size. Even in the case of WM, the difference in J_R curves is not significant regarding the residual strength prediction (tensile panel 83, 3 pt bend specimen N-2). Again,the J_R curve for WM is positioned below the J_R curve for BM, indicating lower crack resistance of WM, as in a previous case (Fig. 3).

The pressure of 170 bar could not produce the extension of initial crack depth a_o = 5 mm (a_o/t = 0.3125) in BM, as one can conclude for BM-2 curve in Fig. 5. Similarly, the pressure of 150 bar will affect only slightly the initial crack depth of a_o = 9.28 mm (a_o/t = 0.58) in BM (specimen 80-1). When the WM is considered, the pressure of 164 bar is required for stable growth of the crack, initially deep 5.44 mm (a_o/t = 0.34), producing crack depth extension to 6.93 mm (point A_1), and the pressure of 150 bar would extend in stable manner the crack of initial depth a_o = 9.12 mm (a_o/t = 0.57) for next 2.61 mm (to 11.73 mm). It is not difficult to conclude that the model can surely withstand even the pressure of 150 bar with the ligament of only 6.88 mm in WM, when the crack is not longer than 64.25 mm. All these results confirmed very high crack growth resistance of SM 80P steel and its SAW WM.

Regarding the applied procedure, two additional problem had occured. The first problem is connected with the shell parameter. According to Eq. (1), the shell parameter depends on pressure vessel diameter, its wall thickness and crack length. For the tensile panel the shell parameter equals zero, because its diameter is infinite, and the crack length has no influence in that case, as one can conclude from Eq. (1). From this standpoint it would be possible to show that J_R curves obtained for flat specimens (tensile panel and 3 pt bend specimen) and applied in residual strength

prediction will not cause a significant error in the results. The second problem, that requires further investigation, is connected with the selection of J_R curve position and initial crack depth a_o value when it is superimposed over crack driving force lines.

J INTEGRAL DIRECT EVALUATION IN THE FULL-SCALE MODEL TEST

The J integral direct evaluation method offers an important improvement in residual strength prediction, since it can be applied in full-scale pressure vessel tests. This method was applied in experiments with the model (Fig. 4). The sample (designed "A" on Fig. 4), was prepared by manual arc welding (MAW), using low-hydrogen basic coated electrode LB-116, produced by "Kobe Steel" - Japan. The undermatching effect was less pronounced with this electrode, producing σ_{YM} = 722 MPa yield strength in WM. The sample was machine notched and pre-cracked by fatigue before its mounting on the model. Fatigue procedure was performed by 3 pt bending in three steps, with different load levels, on two fatigue testing machine, because the crack size after the first loading step was evaluated as inadequate. The sample was mounted by MAW procedure in the window, open in model mantly by cutting. The strain gauges (SG) were positioned, after sample mounting, along properly selected J integral path, on the outer and inner wall side, according to Fig. 4b. The crack mouth opening displacement (CMOD) was followed by a clip gauge.

The experiment was performed in two stages. In the first stage the model was loaded by the following pressure sequences: 0-40-30--50-40-60-50-70-0 bar in the first day, and 0-40-20-60-30-80-40-90--50-100-0 bar in the next day. The SG and CMOD readings were taken during the corresponding holding time at given pressure. Some of the results obtained in this experimental stage are presented in Ref. (6), where it was shown that the J integral direct evaluation is applicable in full-scale pressure vessel tests, allowing further improvements in residual strength prediction. Before the second experimental stage a rough prediction of the pressure level required for model failure was made. Based on the results obtained in Fig. 5 for SAW WM it was expected that the available pump pressure of 134 bar could be sufficient for breaking of the sample ligament of only 4 mm in WM, that was appraised from compliance measurements during fatigue preloading. For the second model loading the following pressure sequence, was prescribed: 0-20-30-40-0-40-60-70-80--0-60-80-90-100-110-115-120-0-90-110-120-125-130-0-134 bar. Since the pump capacity was exhausted and the sample had not been broken, it had been cut out, fatigue loaded in 3 pt bending for marking, and definitely broken by a monotonously rising load.

Typical experimental results, with calculated J integral values, are given in Table 1.

TABLE 1 - Strains along J-integral Path, CMOD's and J-integral Values for different Pressure Levels

Strain gauge μm/m		Pressure p, bar								
		40	60	80	100	110	120	125	130	134
M41	Inner side	12	-46	-463	-722	-876	-614	-318	-612	-1142
M42		360	355	477	473	409	463	501	501	431
M44		152	296	486	587	650	850	924	1000	1050
M45		172	334	542	721	797	934	1024	1119	1151
M46		189	365	598	794	876	1094	1161	1308	1349
M47		561	754	862	842	815	837	659	625	487
M57	Outer side	-102	-211	-321	-409	-436	-462	-419	-426	-374
M56		-89	-183	-292	-365	-405	-427	-391	-422	-372
M55		-87	-197	-299	-380	-424	-463	-457	-503	-466
M53		67	88	87	96	47	47	-31	-79	-125
M52		373	540	703	841	854	875	816	781	747
M51		553	846	1131	1383	1479	1537	1525	1526	1511
M50		791	1193	1584	1948	2094	2226	2285	2319	2361
M49		808	1224	1640	2021	2173	2431	2422	2508	2559
CMOD, μm		537	564	592	623	631	656	686	711	733
Remote stress σ_{yy}, MPa		74	114	182	221	237	269	278	297	295
J integral kN/m		38.2	60.6	104.4	133	146.6	169.2	181.1	202.8	210.4

The hoop stress was calculated from

$$\sigma_{yy} = \frac{E}{1 - \nu^2} (\varepsilon_{yy} + \nu\varepsilon_{zz}) \quad \ldots\ldots\ldots\ldots\ldots\ldots\ldots\ldots \quad (3)$$

with the value ε_{yy} measured on SG 45 and ε_{zz} measured on SG 47, positioned in axial direction, near SG 45. The J integral was calculated from the data given in Table 1, following the procedure, described elsewhere (5), (6).

Hoop stress σ_{yy}, CMOD and J integral are plotted against the pressure in Fig. 6. The overall distribution of given values is similar to that previously obtained (6), but some results must be

compared and analyzed. During the first and second stage of experiment many SG showed continuous redistribution of strains with variation of pressure. The existence of crack, residual stresses and heterogeneity of weldment could be responsible for this redistribution. This was clearly observed in SG 47 and SG 52. The size of the sample was inadequate regarding stress distribution, and influenced significantly the J integral values.

In order to bring more insight, the loading history is considered regarding its influence on the crack propagation (Fig. 7). The fracture surface revealed different marks, connected with the acting load. The fatigue crack (B), that was developed from machined notch (A), is characterized by three visible beach marks (1-2--3). The beach mark 1 corresponds to the fatigue on the first machine, 2 and 3 are obtained during the second fatigue, with different loading levels. Fractured area C is obtained in the first stage of experiment and its final points 4 and 5 were observed at the end of the first stage and denoted on the free outer surface of the wall. From Fig. 7 one can conclude that the crack developed in length, but not in depth. This was additionaly confirmed by the analysis of stretch zone, which spread from the fatigue crack tip. In the deepest point of the crack the stretch zone did not achieve its final size and no crack growth was observed. The same is valid along the segment a-b, that only slightly deflected from a straight line. In the ending points of this segment, the final size of the stretch zone had been achieved, and from these points to the free surface the extension of crack increased gradually. The fractured area D, obtained in the second stage, represents simply the further extension of area C, belonging to the same process of the fracture. The boundary between the first and second stages is only slightly marked. The crack length after the first stage was 74 mm, and after the second stage 80 mm. The area E had been obtained in final fatigue, and area F corresponded to final, ductile fracture. The view of broken tensile panel, given in Fig. 8, shows that in this case the crack propagated in depth, but not in length. This difference in surface crack behaviour in the model and tensile panel requires further consideration.

Turning back to the residual strength prediction, it can be concluded that crack length increase, as observed in the model, will change the shell parameter, and this consequence has to be taken into account. That means, a set of crack driving force lines should be expressed through variable shell parameter and J integral variation should be expressed through the length (and not depth) increase.

The experience, gathered in this full-scale experiment has shown that some improvement in experimental technics has to be required. The sample has to be designed with sufficient size, in order to minimize the secondary residual stress effect of sample mounting. Some of SG, positioned on the inner wall side, were damaged at high pressure (e. g. SG 43, that was not presented in

Table 1) by the water leakage between the wire and insulation. A pump of higher capacity has to be provided. The exagerated difference in remote strain on the same distance (SG M 49 on outer side and SG M 46 on inner side) has to be analyzed; a possible cause could be the inner pressure effect, Khan and Chen (11). The CMOD measurements, obtained with a clip gauge on 10 mm measuring basis, are likely to be overestimated and the introduction of a more precise device has to be considered.

CONCLUSIONS

1. Experimental results of J integral direct evaluation in tensile panels and in full-scale pressure vessel tests can be used for an improvement in residual strength prediction.
2. Additional theoretical and experimental analysis is required for better understanding of different surface crack growth behaviour, observed in tensile panel and full-scale pressure vessel.
3. For the residual strength prediction the part of the lowest crack resistance has to be considered. Hence, experiments have to be extended to HAZ and these results should be compared with the results for WM, that was found to be less resistant than BM.
4. Further experimental improvement is required for the next experiment. The sample size has to be considered for minimization of the residual stress effect. The leakage of inner SG cables at high pressure can require the change in sealing design. The measuring system for strains and CMOD has to be analyzed regarding its correctness.

SYMBOLS USED

a = surface crack depth (mm)

a_o = initial surface crack depth (mm)

2ℓ = surface crack length (mm)

p = pressure (bar)

t = wall thickness (mm)

E = elasticity modulus (GPa)

J = path independent integral (kN/m)

ε_{yy} = strain component in circumferential direction (μm/m)

ε_{zz} = strain component in axial direction (μm/m)

λ = shell parameter

ν = Poisson's ratio

σ_{yy} = hoop stress component (MPa)

σ_Y = yield stress (MPa)

σ_{YB} = yield stress of base metal (MPa)

σ_{YS} = yield stress of submerged arc welding weld metal (MPa)

σ_{YM} = yield stress of manual arc welding weld metal (MPa)

REFERENCES

(1) Satoh, K. and Toyoda, M., "Joint Strength of Heavy Plates with Lower Strength Weld Metal", AWS, 1975.

(2) Rak, I., Gliha, V. and Kuder, J., Metalna-Strokovni bilten '84, No. 1, 1984, pp. 15-23.(in Slovene).

(3) Sedmak, S., Radović, A. and Nedeljković, Lj., "The Strength of Welds in HSLA Steel after Initial Plastic Deformation "Proceedings of ICM 3 Conference on "Mechanical Behaviour of Materials", Edited by K. J. Miller and R. F. Smith, Pergamon Press, Oxford and New York, 1979.

(4) Ratwani, M., Sedmak, S. and Petrovski, B., "Residual Strength Prediction for Pressure Vessels with Surface Flaw using Resistance Curves", Proceedings of the Third Fracture Mechanics Summer School on "Fracture Mechanics of Weldments", Edited by S. Sedmak,Goša-TMF, Beograd, 1985. (in Serbo-Croation).

(5) Read, D. T., "Experimental Method for Direct Evaluation of the J-contour Integral", Proceedings of Fracture Mechanics: Fourteenth Symposium, Vol. II "Testing and Applications", Edited by Lewis and Sines, STP 791, ASTM, Philadelphia, 1983.

(6) Sedmak, S. and Petrovski, B., "The Application of J-integral Direct Measurement on the Pressure Vessel with Axial Notch", presented at the Poster Session on Eighteenth National Symposium on Fracture Mechanics in Boulder, 1985, (submitted for publication).

(7) "Fracture Toughness Evaluation by R-curve Method", STP 527, ASTM, Philadelphia, 1973.

(8) Erdogan, F. and Ratwani, M., Nucl. Eng. and Design 20, 1972, pp. 265-286

(9) Sumpter, J. D. G. and Turner, C. E., "Method for Laboratory Determination of J_{Ic}", Proceedings of Nineth Conference on Cracks and Fracture, STP 601, ASTM, Philadelphia, 1976.

(10) Glavardanov, I., Sedmak, S. and Petrovski, B., "Determination of Crack Resistance Properties of HSLA Steel and its Welded Joint using J-integral", Proceedings of 8th Congress on Material Testing, Vol. II, OMIKK - Technoinform, Budapest, 1982.

(11) Khan, A. S. and Chen, J. C., Ex. Mech. Vol. 25, No. 2, 1985, pp. 123-128.

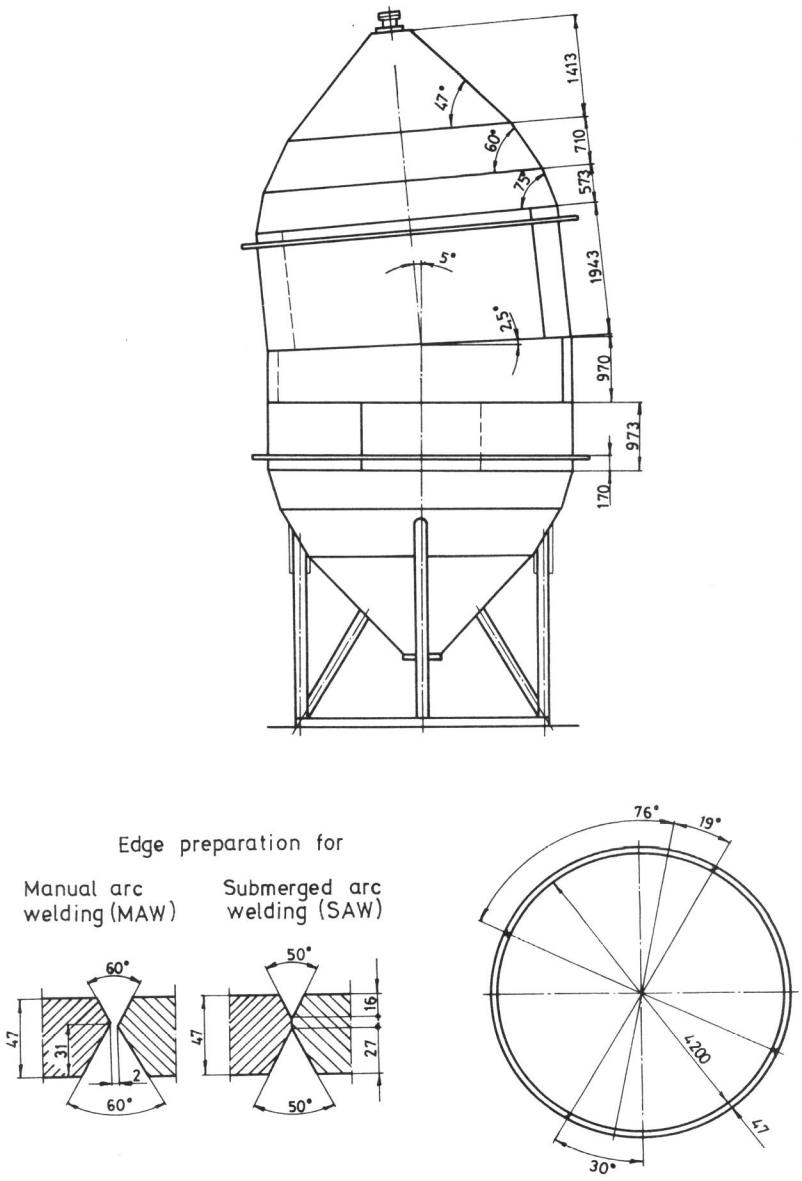

Figure 1. Shape and dimensions of penstock prototype

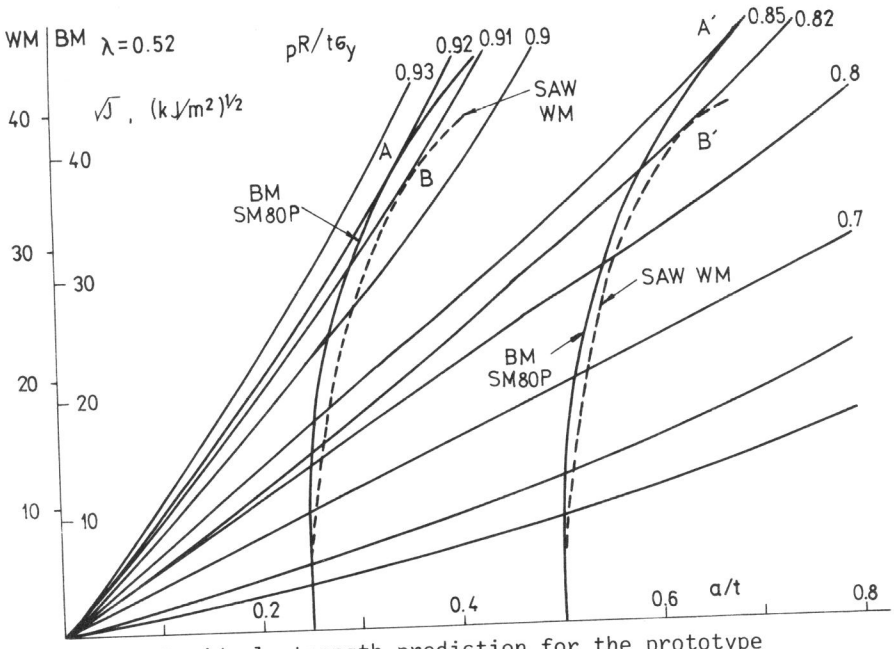

Figure 2. Residual strength prediction for the prototype with an axial crack

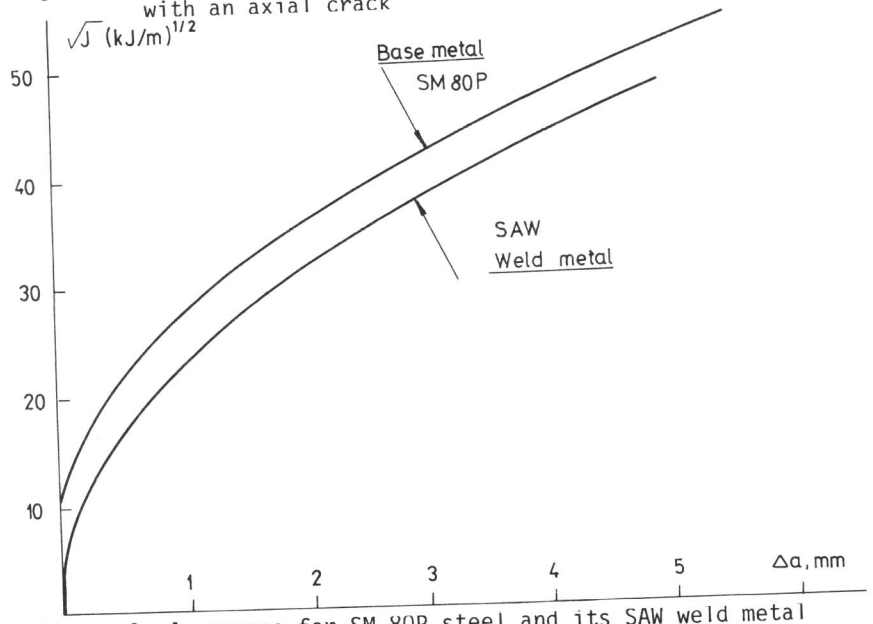

Figure 3. J_R curves for SM 80P steel and its SAW weld metal

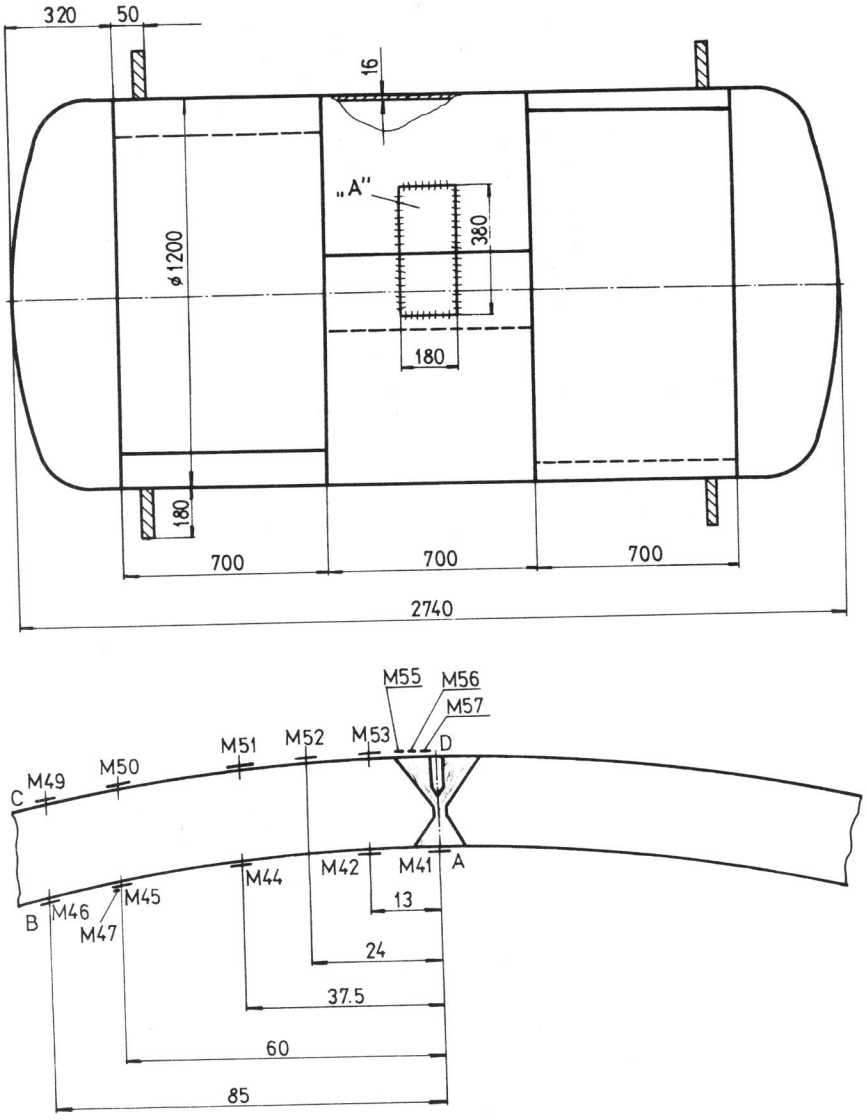

Figure 4. Pressure vessel model and mounted sample "A" with strain gauges disposition

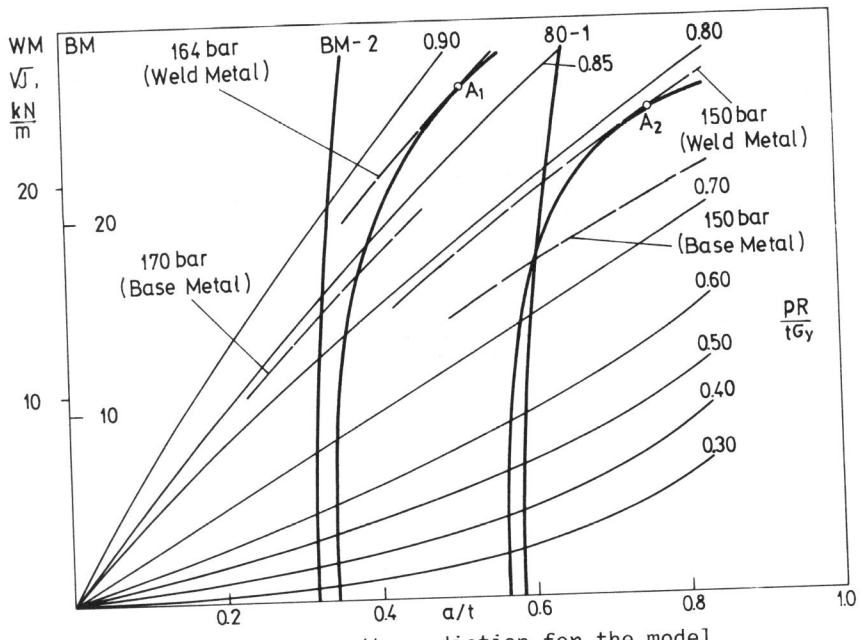

Figure 5. Residual strength prediction for the model with an axial crack

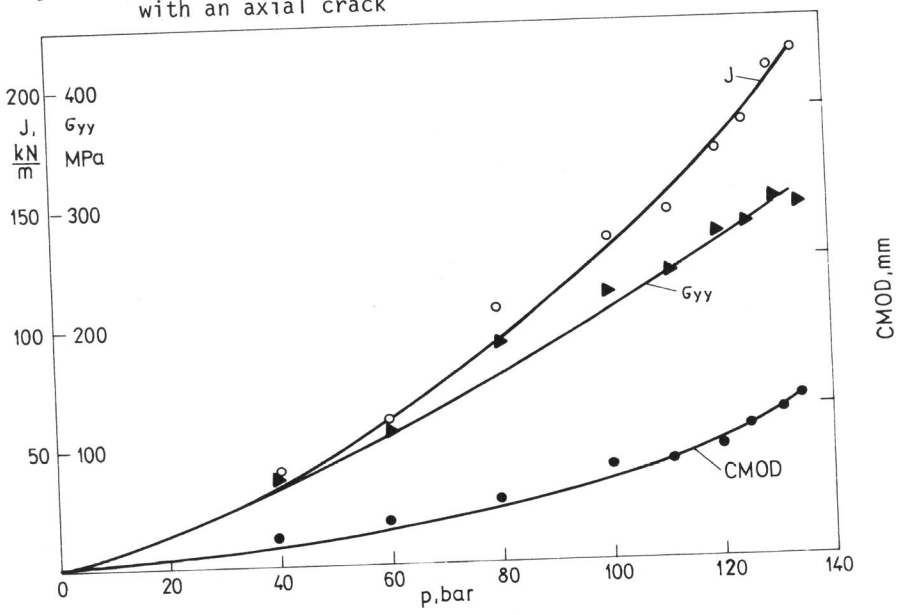

Figure 6. Hoop stress σ_{yy}, CMOD and J integral versus pressure p

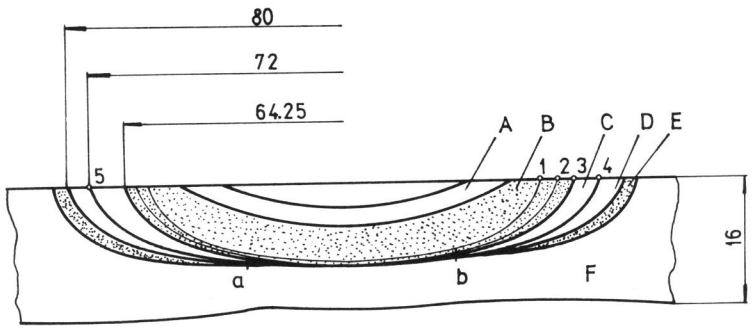

Figure 7. Sheme of model sample fracture surface

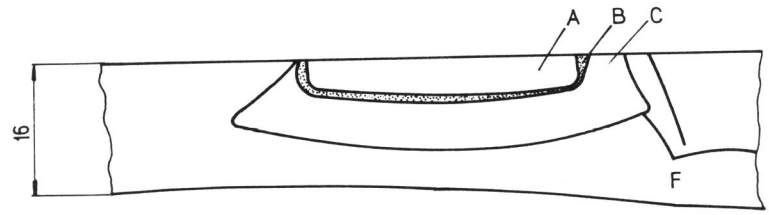

Figure 8. Sheme of tensile panel fracture surface